

Development 136, 1962 (2009) doi:10.1242/dev.038380

Specific regions within the embryonic midbrain and cerebellum require different levels of FGF signaling during development

M. Albert Basson, Diego Echevarria, Christina Petersen Ahn, Anamaria Sudarov, Alexandra L. Joyner, Ivor J. Mason, Salvador Martinez and Gail R. Martin

There was an error published in *Development* **135**, 889-898.

The incorrect image (a duplicate of Fig. S2B') was shown in Fig. S2A' in the supplementary material and has now been corrected. The findings of this experiment remain unchanged.

The authors apologise to readers for this mistake.

Specific regions within the embryonic midbrain and cerebellum require different levels of FGF signaling during development

M. Albert Basson^{1,2,3,*}, Diego Echevarria^{4,*}, Christina Petersen Ahn^{1,*}, Anamaria Sudarov⁵, Alexandra L. Joyner⁵, Ivor J. Mason², Salvador Martinez⁴ and Gail R. Martin^{1,†}

Prospective midbrain and cerebellum formation are coordinated by FGF ligands produced by the isthmic organizer. Previous studies have suggested that midbrain and cerebellum development require different levels of FGF signaling. However, little is known about the extent to which specific regions within these two parts of the brain differ in their requirement for FGF signaling during embryogenesis. Here, we have explored the effects of inhibiting FGF signaling within the embryonic mouse midbrain (mesencephalon) and cerebellum (rhombomere 1) by misexpressing sprouty2 (*Spry2*) from an early stage. We show that such *Spry2* misexpression moderately reduces FGF signaling, and that this reduction causes cell death in the anterior mesencephalon, the region furthest from the source of FGF ligands. Interestingly, the remaining mesencephalon cells develop into anterior midbrain, indicating that a low level of FGF signaling is sufficient to promote only anterior midbrain development. *Spry2* misexpression also affects development of the vermis, the part of the cerebellum that spans the midline. We found that, whereas misexpression of *Spry2* alone caused loss of the anterior vermis, reducing FGF signaling further, by decreasing *Fgf8* gene dose, resulted in loss of the entire vermis. Our data suggest that cell death is not responsible for vermis loss, but rather that it fails to develop because reducing FGF signaling perturbs the balance between vermis and roof plate development in rhombomere 1. We suggest a molecular explanation for this phenomenon by providing evidence that FGF signaling functions to inhibit the BMP signaling that promotes roof plate development.

KEY WORDS: FGF, Midbrain, Cerebellum, Sprouty, Apoptosis, Vermis, Roof plate

INTRODUCTION

Remarkable progress has been made in understanding how the development of anatomically and functionally distinct subdivisions of the vertebrate brain is controlled. Midbrain and cerebellum formation has been particularly well studied (Raible and Brand, 2004; Zervas et al., 2005). The midbrain develops from the mesencephalon (mes) (see Fig. 1D). The dorsal mes gives rise to the tectum, which comprises the superior colliculus (SC) anteriorly and inferior colliculus (IC) posteriorly, where visual and auditory stimuli are processed, respectively. The cerebellum develops from dorsal rhombomere 1 (r1): the anterior-most segment of the hindbrain (see Fig. 1D). In mouse, the cerebellum consists of a medial vermis, flanked laterally by a pair of hemispheres (see Fig. 1E). The cerebellum, where motor activity is coordinated, undergoes dramatic changes after birth that transform it into a highly foliated structure (Sillitoe and Joyner, 2007). The molecular mechanisms that subdivide the tectum and cerebellum into subregions are poorly understood.

At early stages, signals that pattern both mes and r1 are produced by a signaling center, the isthmic organizer (IsO), at the mes/r1 boundary (Echevarria et al., 2003; Nakamura et al., 2005; Partanen,

2007), thereby ensuring coordination of midbrain and cerebellum development. One key component of the IsO signal is FGF8 (Crossley et al., 1996), a member of the fibroblast growth factor (FGF) family (Itoh and Ornitz, 2004). In mouse, *Fgf8* is expressed in r1 from early neural plate [embryonic day (E) 8.25] through mid-gestation (E12.5) stages. By E10.0, *Fgf8* expression is localized in r1, just posterior to the mes/r1 boundary, in a circular domain that is interrupted by *Fgf8*-negative regions at the dorsal and ventral midlines (roof and floor plates, respectively) (Crossley and Martin, 1995). When *Fgf8* is inactivated in the early neural plate, all mes and r1 cells die between E8.5 and E10. However, when *Fgf8* expression is only moderately reduced, the anterior midbrain appears normal, but posterior midbrain, isthmus and vermis are lost (Chi et al., 2003). The reason for such tissue loss in *Fgf8* hypomorphs is unknown.

FGF8 regulates the expression of *Fgf17* (Chi et al., 2003), which is detected in a broad domain encompassing both prospective posterior midbrain and cerebellum (Xu et al., 2000). In *Fgf17*-null mice, part of the IC and anterior vermis are absent, but the remaining midbrain and cerebellum appear normal. The extent of vermis loss is increased in these mutants by removing one copy of *Fgf8*, suggesting that the two FGF family members cooperate to control cerebellum development (Xu et al., 2000).

The level of FGF signaling can affect cell fate during mes/r1 development. Ectopic expression of an *Fgf8* splice variant, *Fgf8b*, which encodes an FGF8 isoform with high affinity for FGF receptors (Olsen et al., 2006), transforms mouse mes cells to a cerebellar fate (Liu et al., 1999). By contrast, ectopic expression of *Fgf8a*, which encodes an FGF8 isoform with much lower affinity for FGF receptors (Olsen et al., 2006; Zhang et al., 2006), expands the mes and transforms posterior forebrain (diencephalon) progenitors to a midbrain fate (Lee et al., 1997; Liu et al., 1999).

¹Department of Anatomy and Program in Developmental Biology, University of California, San Francisco, CA 94158, USA. ²MRC Centre for Developmental Neurobiology, King's College London, London SE1 1UL, UK. ³Department of Craniofacial Development, King's College London, London SE1 9RT, UK. ⁴Instituto de Neurociencias de Alicante, UMH-CSIC, 03550-San Juan de Alicante, Spain. ⁵Developmental Biology Program, Memorial Sloan-Kettering Cancer Center, New York, NY 10021, USA.

*These authors contributed equally to this work

†Author for correspondence (e-mail: gail.r.martin@ucsf.edu)

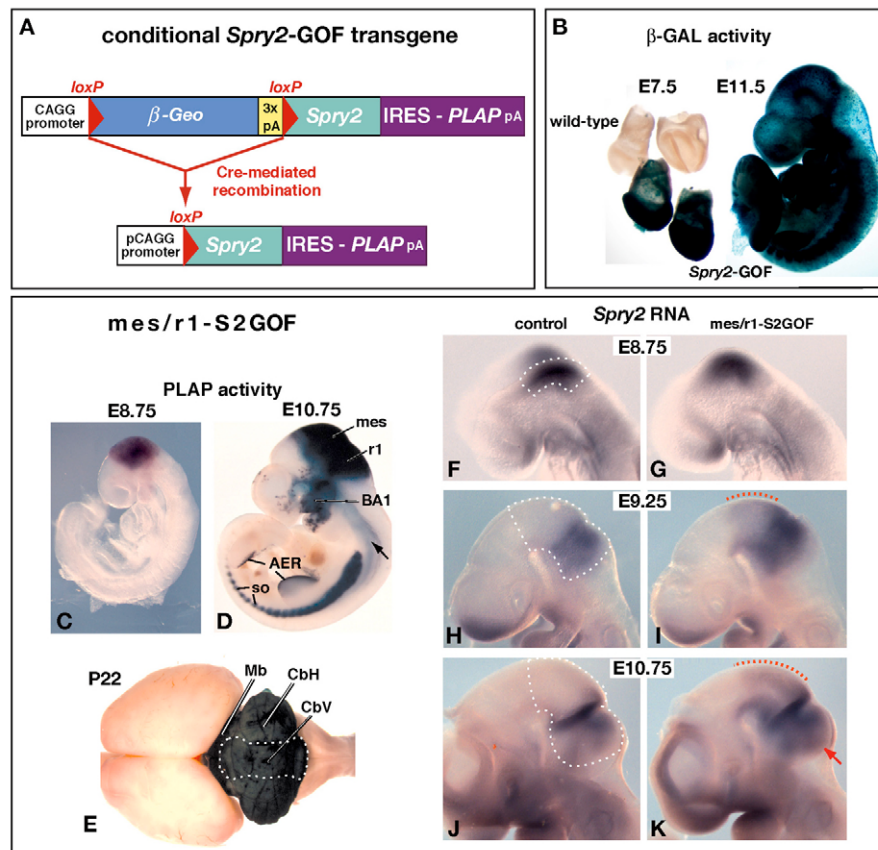


Fig. 1. *Spry2*-GOF, a conditional *Spry2* gain-of-function allele, and its expression following recombination by *En1*^{Cre}. (A) Schematic diagram illustrating the *Spry2*-GOF transgene. The CAGG promoter drives expression of the β -Geo gene, which is followed by a triple polyadenylation sequence (3 \times pA). Cre-mediated recombination deletes β -Geo, and mouse *Spry2* and human placental alkaline phosphatase (PLAP) cDNAs are expressed as a bicistronic mRNA containing an internal ribosome entry site (IRES) that directs translation of PLAP. (B) Assays in whole mount for β -Geo expression (β -GAL activity) in embryos hemizygous for *Spry2*-GOF. (C–K) Analysis of expression of the recombined *Spry2*-GOF transgene in *En1*^{Cre/+}; *Spry2*-GOF (*mes/r1-S2GOF*) mutants. (C–E) Assays for PLAP activity in embryos and postnatal brain at the stages indicated. Blue staining identifies cells in which recombination of the transgene occurred. The arrow in D indicates two ventrolateral stripes in the spinal cord. (F–K) RNA in situ hybridization assays in whole mount at the stages indicated, using a mouse *Spry2* probe. The broken white lines outline the left side of *mes/r1* in the control embryos, where the probe detects endogenous *Spry2* expression. In *mes/r1-S2GOF* embryos, the *Spry2* RNA detected represents the sum of expression from the endogenous *Spry2* gene and the recombined transgene. Regions in which there is ectopic *Spry2* expression in *mes* and in *r1* are indicated by broken red lines (I,K) and by a red arrow (K), respectively. AER, apical ectodermal ridge of the limb bud; BA1, first branchial arch; CbV, cerebellar vermis; CbH, cerebellar hemispheres; Mb, midbrain; *mes*, mesencephalon; *r1*, rhombomere 1; *so*, somites.

Importantly, when *Fgf8b* is ectopically expressed at low rather than high level in chicken embryos, the results are similar to those obtained with *Fgf8a* or *Fgf17*. Together, these data indicate that specification of midbrain and cerebellum require different levels of FGF signaling (Sato et al., 2001; Liu et al., 2003), and highlight the importance of controlling FGF signaling during *mes/r1* development.

Such control can be achieved intracellularly by sprouty proteins (Hacohen et al., 1998; Casci et al., 1999), the expression of which is induced by signaling through FGF receptors (FGFRs) and other receptor tyrosine kinases (RTKs) (Mason et al., 2006). There are four sprouty genes in mouse and human. *Spry1* and *Spry2* are strongly expressed in *mes/r1* from early neural plate stages, in cells near the IsO (Minowada et al., 1999). In zebrafish (Furthauer et al., 2001) and chicken (Suzuki-Hirano et al., 2005) embryos, increasing sprouty gene expression above normal levels can antagonize FGF activity and interfere with *mes/r1* development.

Recent studies have demonstrated that the roof plate in *r1* is another important source of signals, including BMP ligands, for cerebellar development (Chizhikov et al., 2006; Machold et al., 2007). Roof plate development itself is controlled by *Lmx1a* (Millonig et al., 2000), a gene positively regulated by BMP signaling (Chizhikov and Millen, 2004a; Chizhikov et al., 2006). It is not known whether signals emanating from the IsO affect the development or function of the cerebellar roof plate or vice versa.

Here, we have employed a mouse line carrying a conditional *Spry2* gain-of-function transgene in conjunction with an *Fgf8*^{null} allele to produce the equivalent of an FGF loss-of-function allelic series specifically in *mes/r1*. By studying the phenotypic effects of these genetic manipulations, we have uncovered potential mechanism(s) by which FGF signaling differentially regulates the development of specific regions within the midbrain and cerebellum.

MATERIALS AND METHODS

Genotyping

All mutant alleles were maintained on a mixed genetic background. Genotypes were determined by PCR assays using embryonic yolk sac or tail DNA as a template. The *Spry2*-GOF allele (Calmont et al., 2006), which was produced essentially as described by Lu et al. (Lu et al., 2006), was detected using primers that amplify human *PLAP* (*ALPP*). *Spry2* gain-of-function homozygotes were identified using a quantitative PCR assay for *PLAP* sequences (primers and conditions available upon request). Other alleles were detected as previously described: *En1^{Cre}* and *Fgf8^{null}* (Chi et al., 2003); *Fgf8^{neo}* (Sun et al., 1999); and *Fgf17* (Xu et al., 2000).

Histological analysis and assays for cell death and gene expression

Noon of the day when a vaginal plug was detected was considered E0.5. Embryos were staged more precisely by counting somites posterior to the forelimb bud and scoring the first one counted as somite 13. Histological analysis of late gestation and postnatal brains, and immunolocalization in brain tissue were performed as previously described (Chi et al., 2003).

Assays for cell death were performed in whole mount by staining with LysoTrackerT (Molecular Probes L-7528), as previously described by Grieshammer et al. (Grieshammer et al., 2005). We confirmed that LysoTrackerT staining gave results on *En1^{Cre/+};Fgf8^{lox/-}* (referred to here as mes/r1-*Fgf8*-KO) embryos similar to those we previously obtained using Nile Blue Sulfate staining and TUNEL assays to detect cell death (Chi et al., 2003).

For gene expression analysis, embryos were collected in cold PBS, fixed in 4% paraformaldehyde and stored in 70% ethanol at -20°C . Some embryos were embedded in paraffin and sectioned at 7 μm . Standard protocols were employed for RNA in situ hybridization on sections and in whole mount, and for assaying β -GAL and PLAP activity in whole mount.

RESULTS

Cre-mediated recombination of a conditional *Spry2* gain-of-function transgene in midbrain and cerebellum progenitors

To reduce FGF signaling in mes/r1, we employed a mouse line carrying a conditional *Spry2* gain-of-function allele, *Spry2*-GOF (Calmont et al., 2006). In these mice, transgene-expressing cells produce β -GEO, a fusion protein with both neomycin-resistance and β -galactosidase (β -gal) activities (Friedrich and Soriano, 1991) (Fig. 1A). β -Gal assays demonstrated that *Spry2*-GOF is expressed in most cells of the embryo from E7.5 to at least E11.5 (Fig. 1B, and data not shown). Cells in which the transgene has undergone Cre-mediated recombination express a bicistronic mRNA containing both *Spry2*- and human placental alkaline phosphatase (*PLAP*)-coding sequences (Fig. 1A). PLAP protein thus functions as a convenient reporter for expression of the recombined transgene.

To obtain mice in which the transgene was recombined in mes/r1, we crossed animals carrying *Spry2*-GOF and *En1^{Cre}*, an *En1* allele with *cre* inserted in the first exon (Kimmel et al., 2000). In their *En1^{Cre/+};Spry2*-GOF offspring, we detected PLAP activity only in the domains in which *En1^{Cre}* is known to function (Li et al., 2002; Chi et al., 2003). Thus, in the developing brain, no PLAP activity was detected prior to E8.25 (not shown), but strong PLAP activity was observed throughout mes/r1 from E8.75 (Fig. 1C). Subsequently, because the CAGG promoter remains active in most embryo and adult cells, PLAP activity was detected throughout the mes and r1 at E10.75 (Fig. 1D), and the midbrain and cerebellum on postnatal day (P) 22 (Fig. 1E). In addition, by E10.75, PLAP activity was detected in the first branchial arch (Fig. 1D), presumably in mes/r1-derived neural crest cells that continue to express the recombined *Spry2*-GOF transgene under the control of the CAGG promoter. PLAP activity was also detected in other domains in which *En1* is normally

expressed (Kimmel et al., 2000) (Fig. 1D). No PLAP activity was detected in control littermates (wild type or mutants carrying only *En1^{Cre/+}* or only *Spry2*-GOF; not shown). *En1^{Cre/+};Spry2*-GOF mutants will hereafter be referred to as mes/r1-S2GOF embryos, to indicate that the recombined transgene was expressed in mes/r1.

To assess *Spry2* expression directly from the recombined transgene, we performed a whole-mount RNA in situ hybridization analysis on mes/r1-S2GOF mutants and control littermates. Consistent with previous studies (Minowada et al., 1999), in control embryos we detected *Spry2* RNA at E8.75 in a domain encompassing most of mes/r1 (Fig. 1F), which subsequently became progressively more restricted, such that by E9.25 and at E10.75 it encompassed the posterior mes and r1 but not the anterior mes (Fig. 1H,J). In mes/r1-S2GOF mutants at these stages (Fig. 1C,D), the level of *Spry2* RNA appeared to be only slightly increased within the normal domains of *Spry2* expression (Fig. 1G,I,K). However, because transgene expression persisted in regions where *Spry2* expression is normally downregulated, we detected ectopic *Spry2* expression in anterior mes and posterior r1 at later stages (E9.25 and E10.75; Fig. 1I,K). In situ hybridization analysis on sections of mes/r1-S2GOF mutants at 42 somites demonstrated that *Spry2* RNA was distributed uniformly within the ectopic expression domain (not shown). Together, our data suggest that in mes/r1-S2GOF embryos, the level of *Spry2* RNA is slightly elevated within its normal expression domain and is ectopically expressed throughout the remainder of the developing midbrain and cerebellum from at least E8.75.

Similar effects on midbrain and cerebellum are obtained by expressing one copy of recombined *Spry2*-GOF in mes/r1 or by reducing *Fgf17* and *Fgf8* gene dose

Histological analysis of mes/r1-S2GOF mutants shortly before birth revealed the effects of expressing the recombined transgene on midbrain and cerebellum development. In midsagittal sections of E17.5 mes/r1-S2GOF mutants ($n=4$), the dorsal midbrain appeared normal at its anterior end, some tissue loss was observed at the posterior end of the SC, and the IC was absent (Fig. 2A,B; data not shown). Staining for calretinin confirmed the absence of the IC, which is normally calretinin-negative (Fig. 2C,D). Posterior to the midbrain, the dorsal isthmus was also absent (Fig. 2A-D). The medial cerebellum (vermis) also appeared to have lost tissue, but only at its anterior end (Fig. 2A,B, and data not shown). By contrast, basal plate derivatives in the midbrain [oculomotor nucleus (nIII), substantia nigra and ventral tegmental area (SN-VTA)], and the isthmus [trochlear nucleus (nIV)], were present, as was the r1-derived locus coeruleus, and all appeared normal (not shown).

Mes/r1-S2GOF mutants were viable, and lacked the IC and isthmus postnatally (Fig. 2G,H), demonstrating that the apparent tissue loss observed at E17.5 was not due to a developmental delay. In wild-type mice, there are strain-specific variations in vermis foliation pattern, such that some strains have three distinct lobules (I, II and III) anterior to the lobule of culmen (IV-V), and other strains have only two (indicated as I-II and III in Fig. 2G) (Inouye and Oda, 1980). In postnatal mes/r1-S2GOF mutants ($n=5$), lobules I-III were either reduced or absent, whereas the remaining lobules appeared essentially normal (Fig. 2H; data not shown). Thus, expressing a single copy of the recombined *Spry2*-GOF transgene in mes/r1 from an early developmental stage resulted in absence of the posterior dorsal midbrain (IC), isthmus and anterior vermis. There were no obvious abnormalities in these animals in other tissues that developed from cells in which the *Spry2*-GOF transgene underwent Cre-mediated recombination.

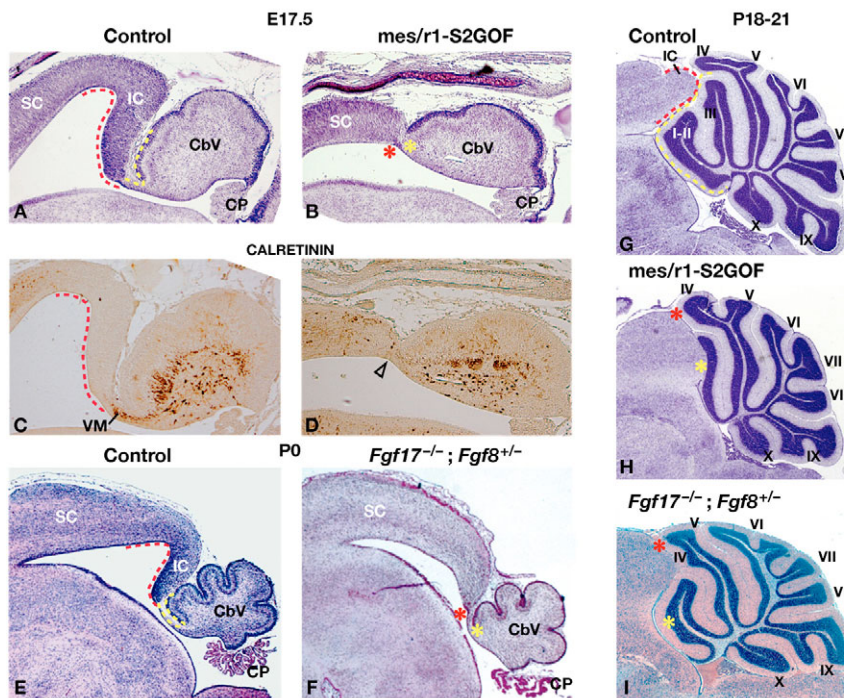


Fig. 2. Expression of a single copy of the recombinated *Spry2*-GOF allele in *mes/r1* causes absence of the inferior colliculus and anterior vermis. (A,B,E-I) Midsagittal sections of brains of the genotypes indicated, collected at the stages denoted and stained with Cresyl Violet or Hematoxylin and Eosin (I). Anterior is towards the left, posterior is towards the right. In control embryos, the posterior midbrain and anterior hindbrain regions that are absent in the mutant embryos are demarcated by red and yellow broken lines, respectively; in the mutant embryos, the regions where the missing midbrain and anterior hindbrain tissue would normally be found are indicated by red and yellow asterisks, respectively. (C,D) Higher power view of the tissue shown in A and B, respectively, stained with an antibody against calretinin (CR). The CR-negative inferior colliculus in the control is indicated by a broken red line. In the mutant, this CR-negative region, as well as the isthmus and velum medullare are absent (arrowhead). (G-I) Comparison of vermis development in control, *mes/r1*-S2GOF, and *Fgf17*^{-/-}; *Fgf8*^{+/-} animals at ~3 weeks of age. CP, choroid plexus; IC, inferior colliculus; SC, superior colliculus; VM, velum medullare. The lobules of the vermis are indicated by Roman numerals, as described by Inouye and Oda (Inouye and Oda, 1980).

The phenotype of *mes/r1*-S2GOF mutants described above is remarkably similar to, although slightly more severe than, that observed in *Fgf17*-null homozygotes carrying one copy of an *Fgf8* null allele (*Fgf17*^{-/-}; *Fgf8*^{+/-} animals) (Xu et al., 2000). At birth, the IC, isthmus and anterior tissue in the developing cerebellum appeared to be absent in such compound FGF mutant animals (Fig. 2E,F), and at 3-4 weeks after birth, only one major lobule was present anterior to lobules IV-V (Fig. 2I). These results suggest that expressing a single copy of the recombinated *Spry2*-GOF allele results in a reduction in FGF signaling during midbrain and cerebellar development to approximately the same degree as in *Fgf17*^{-/-}; *Fgf8*^{+/-} mutants.

Reducing *Fgf8* gene dose in *mes/r1*-S2GOF mutants or expressing two copies of the recombinated *Spry2*-GOF allele in *mes/r1* results in loss of the cerebellar vermis

If expression of the recombinated *Spry2*-GOF allele in *mes/r1* does indeed function to reduce FGF signaling, one might expect that reducing it even further, for example by reducing *Fgf8* gene dose, would result in a more severe phenotype. To test this prediction, we examined *En1*^{Cre/+}; *Spry2*-GOF; *Fgf8*^{+/-} (*mes/r1*-S2GOF;F8) mutants at E17.5. When viewed in whole mount, it was evident that they lacked the entire vermis (Fig. 3A,B). Histological analysis showed that only the anterior region of the dorsal midbrain, including the anterior-most *mes*-derived structure, the PPT (Lagares et al., 1994), appeared normal; tissue was missing at the posterior end of the SC; and the IC, dorsal isthmus and vermis were absent (Fig. 3C-E). *mes/r1*-S2GOF;F8 mutants could be classified in two groups: group I (*n*=3/5) had some tissue loss at the posterior end of the SC, and basal structures including nIII, nIV and the SN-VTA were present although somewhat reduced; group II (*n*=2/5) had more tissue loss at the posterior end of the SC and the basal structures were absent (Fig. 3C-K). Lateral *r1*-derived tissue was present in both groups, as evidenced by the presence of the locus coeruleus, but it was clearly reduced in group II (Fig. 3I-K).

We next examined animals carrying *En1*^{Cre/+} and two copies of the *Spry2*-GOF (*mes/r1*-S2GOF;S2GOF; *n*=3), which appeared similar to *mes/r1*-S2GOF;F8 mutants in group I (not shown). Thus, expressing a second copy of the recombinated *Spry2*-GOF allele appeared to inhibit FGF signaling to approximately the same extent as removing one copy of the *Fgf8* gene in *mes/r1*-S2GOF animals. The phenotype of the group I *mes/r1*-S2GOF;F8 and *mes/r1*-S2GOF;S2GOF mutants is similar to that observed in embryos homozygous for *Fgf8*^{neo} (Chi et al., 2003), a hypomorphic allele of *Fgf8*, that has been estimated to express *Fgf8* RNA at ~40% of the level in wild-type embryos (Meyers et al., 1998). Unlike *Fgf8*^{neo/neo} animals, which have numerous developmental abnormalities caused by reduced FGF8 signaling in all tissues and die at birth, several *mes/r1*-S2GOF;F8 and *mes/r1*-S2GOF;S2GOF mutants survived to adulthood. Thus, we were able to determine the postnatal consequences of the midbrain and cerebellum defects that were detected just before birth. In P21 *mes/r1*-S2GOF;F8 animals, a complete loss of vermis was readily observed in intact brains, whereas the cerebellar hemispheres were present, but appeared somewhat reduced (Fig. 3L,M). Section analysis at P28 revealed a hemisphere-like foliation pattern in lateral sections and further showed that the granule cell layer was of normal thickness; staining with calbindin demonstrated that the density of Purkinje cells was apparently normal, as were their axon and dendrite projections (see Fig. S1 in the supplementary material). Consistent with the absence of the vermis, the Fastigial nucleus was absent, whereas the Dentate nucleus appeared relatively unaffected (not shown). The lack of vermis, which controls posture and locomotion, presumably explains our finding that *mes/r1*-S2GOF;F8 mutants exhibited a widened gait and pronounced ataxia that increased in severity with age (not shown).

Cell death occurs in the anterior mesencephalon in *Spry2*-GOF mutants and *Fgf8* hypomorphs

We have previously shown that eliminating *Fgf8* function in *mes/r1* causes extensive cell death between the 11 and 28 somite stages, resulting in complete absence of the midbrain, isthmus and

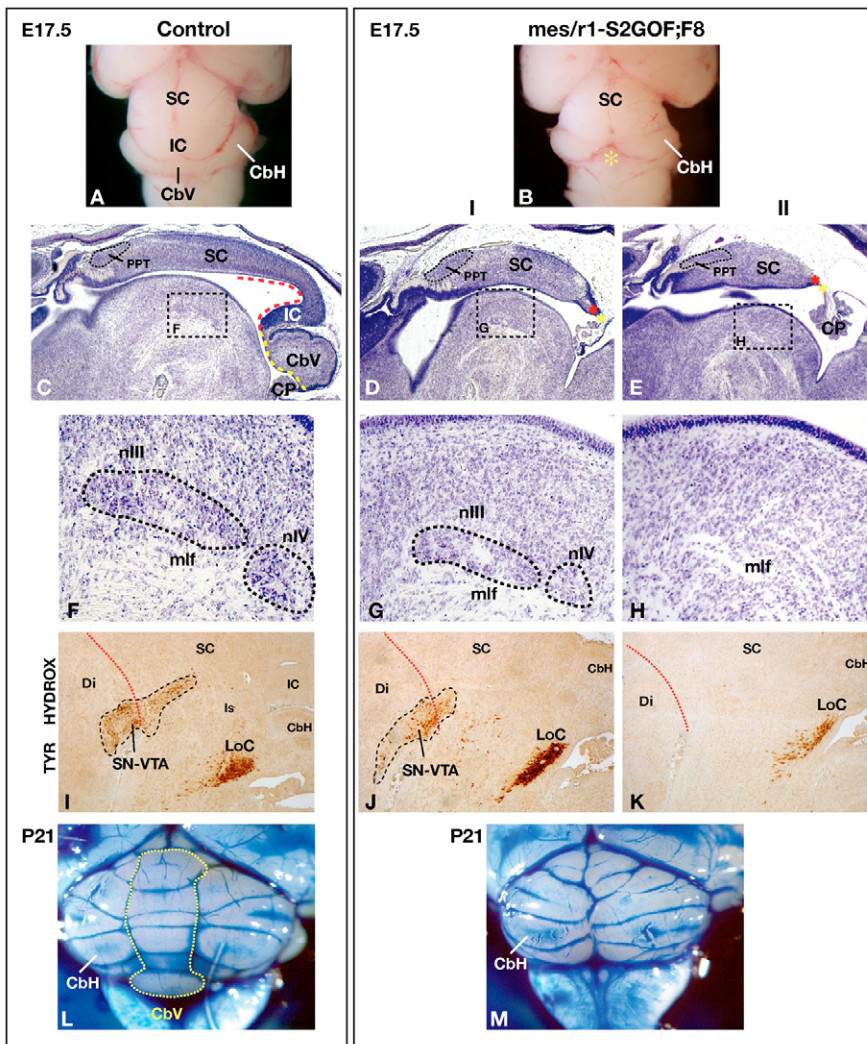


Fig. 3. Decreasing *Fgf8* gene dose in *mes/r1-S2GOF* embryos results in absence of the vermis. (A,B) Dorsal views of brains collected from E17.5 embryos of the genotypes indicated. In the mutant brain, the region where the vermis would normally be found is indicated by a yellow asterisk. (C-E) Low-magnification views of midsagittal sections of E17.5 control and *mes/r1-S2GOF;F8* mutants, stained with Cresyl Violet. (D,E) Examples of the group I (milder) and group II (more severe) brain phenotypes observed in the mutants. The broken red and yellow lines and red and yellow asterisks are explained in the legend to Fig. 2A,B,E,F. The areas outlined in C-E are shown at higher magnification in F-H, respectively. (F-H) High magnification views of basal structures. When present, nIII and nIV are circled with broken lines. (I-K) High magnification views of more lateral sagittal sections of the same brains, assayed by immunohistochemistry with an antibody against tyrosine hydroxylase, which specifically stains nuclei in the lateral posterior diencephalon, midbrain and anterior hindbrain. The broken red line indicates the boundary between diencephalon and midbrain. (L,M) Dorsal views of intact brains collected from P21 mice of the genotypes indicated, stained with ink. The broken line in L outlines the vermis, which is absent in the mutant brain. CbV, cerebellar vermis; CbH, cerebellar hemispheres; CP, choroid plexus; Di, diencephalon; IC, inferior colliculus; Is, isthmus; LoC, locus ceruleus; mlf, medial longitudinal fascicle; nIII, oculomotor nucleus; nIV, trochlear nucleus; PPT, posterior pretectal nucleus; SC, superior colliculus; SN-VTA, substantia nigra-ventral tegmental area.

cerebellum (Chi et al., 2003). However, the effects of only moderately reducing the level of FGF gene expression on cell survival in *mes/r1* were not examined. We therefore sought to determine whether abnormal cell death could account for the tissue loss in embryos that were homozygous for *Fgf8^{neo}* or that expressed the recombined *Spry2-GOF* transgene, by staining with LysotrackerT (see Materials and methods) at 4- to 6-hour intervals between E8.75 and E10.75 (12 to 38 somites).

We detected a relatively small domain in *Fgf8^{neo/neo}* and *mes/r1-S2GOF* mutants in which cell death was more extensive than in controls, but only at the 15- to 16-somite and 18- to 20-somite stages, respectively. A similar domain of abnormal cell death was observed at 18- to 20-somites in *mes/r1-S2GOF;F8* mutants, in which the level of FGF signaling is lower than in *mes/r1-S2GOF* mutants. Surprisingly, given that the anterior midbrain appears to develop normally in all these mutants (Fig. 2A,B; Fig. 3C-E) (Chi et al., 2003), the domain of abnormal cell death was localized at the anterior end of the dorsal mes (Fig. 4A-E; data not shown). To confirm the location of this abnormal cell death, we performed an in situ hybridization assay on the LysotrackerT-labeled embryos using a probe for *Pax6*. This gene is expressed throughout the prospective forebrain, with the posterior limit of its expression domain defining the boundary between the developing diencephalon (di) and mes. The domain

of abnormal cell death, as detected by LysotrackerT staining, was indeed localized immediately posterior to the di/mes boundary (Fig. 4C,C', and data not shown).

One explanation for the abnormal cell death in the mutants is that a certain level of FGF signaling from the IsO is required for cell survival, and that it falls below that level in the anterior mes when either *Spry2* is ectopically expressed or *Fgf8* expression is reduced (as in *Fgf8^{neo/neo}* embryos). To investigate this hypothesis, we determined the range of FGF signaling in *mes/r1* by assaying for *Spry1* expression, which is induced by and thus serves as a reporter for a high level of FGF signaling (Liu et al., 2003; Olsen et al., 2006). We found that at the 18- to 20-somite stage, the distance from the isthmus constriction to the anterior limit of the *Spry1* expression domain was reduced in *mes/r1-S2GOF* and *mes/r1-S2GOF;F8* mutants compared with that in control embryos (Fig. 4F-H). These data provide evidence that the range of FGF signaling from the IsO is decreased in the mes of these mutants, supporting the hypothesis that the observed anterior cell death is a consequence of reduced FGF signaling.

Similar results were obtained in assays for *En1*, *En2* and *Efna2* expression (Fig. 4 and data not shown). At 33-35 somites, the *Efna2* expression domain was smaller than normal in *mes/r1-Spry2-GOF* and even smaller in *mes/r1-Spry2-GOF;F8* embryos (Fig. 4I-K). These data are consistent with studies showing that *En1* and *En2*

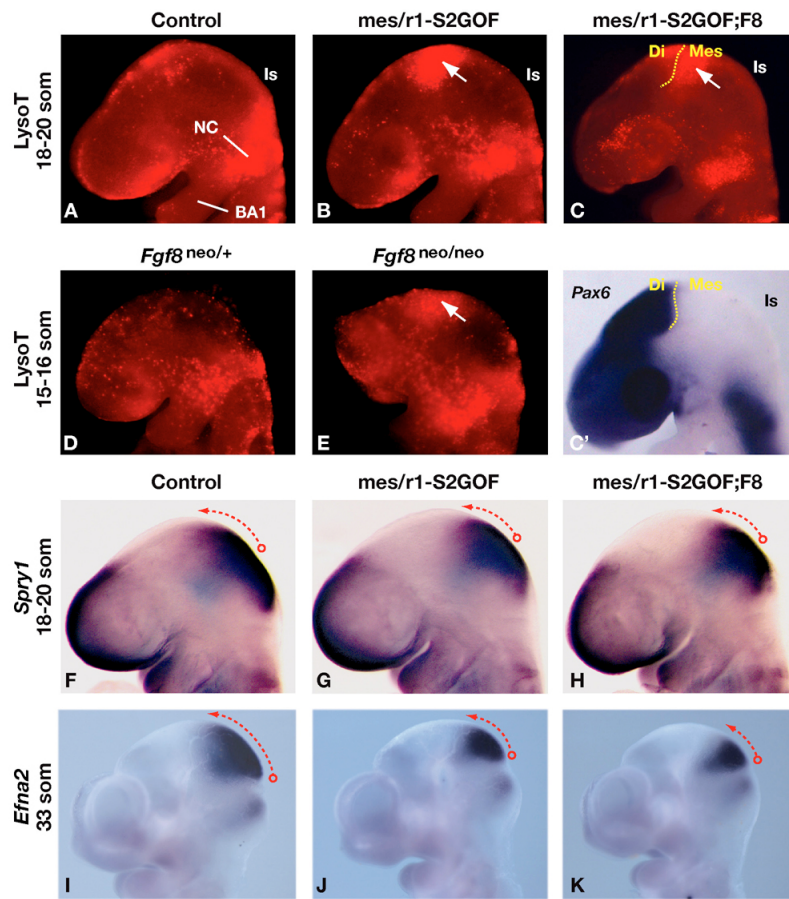


Fig. 4. Reducing FGF signaling from the isthmus organizer results in cell death in the anterior mesencephalon. (A-E) Lateral views of embryos of the genotypes indicated, collected at the somite stages denoted and labeled with LysoTrackerT (LysoT), which marks regions in which dead cells are abundant. The approximate position of the isthmus constriction (Is) is indicated. (C') The embryo shown in C was fixed after labeling with LysoT and assayed by RNA in situ hybridization for *Pax6* expression. The broken yellow line indicates the posterior limit of *Pax6* expression, which lies at the border between the prospective forebrain (diencephalon, Di) and midbrain (mesencephalon, Mes). In control embryos (A,D), LysoT labeling is detected where neural crest (NC) is migrating into the first branchial arch (BA1), but there is relatively little labeling in the neuroepithelium. By contrast, in the mutant embryos (B,C,E) there is extensive LysoT labeling in the mes (white arrows). (F-K) Embryos of the genotypes indicated, collected at the somite stages indicated, were assayed in whole mount by RNA in situ hybridization using a probe for *Spry1* or *Efn2*. The extent of the expression domain from the *mes/r1* boundary (red circle) towards the forebrain is indicated by a broken red arrow.

expression is regulated by FGF signaling (Trokovic et al., 2003), and that ephrin gene expression is controlled by engrailed genes (Nakamura, 2001). In addition, as expected for mutants with reduced FGF signaling from the IsO (Zervas et al., 2005; Partanen, 2007), we found that the posterior limit of *Otx2* expression was slightly less sharp in *mes/r1-S2GOF;F8* mutants than in controls, and a few scattered *Otx2*-positive cells were detected in r1. Furthermore, *Gbx2* and *Wnt1* expression were significantly reduced in anterior r1 and the posterior midbrain, respectively (see Fig. S2 in the supplementary material).

The roof plate is expanded in anterior rhombomere 1 in *mes/r1-S2GOF;F8* mutants

Importantly, in the experiments described above we detected no abnormal cell death in the prospective posterior midbrain or cerebellum of *mes/r1-S2GOF* or *mes/r1-S2GOF;F8* mutants (Fig. 4A-C; data not shown), suggesting that the loss of IC, isthmus and vermis in these mutants is not due to cell death between E8.75 and E11.5. An alternative explanation for the loss of vermis in *mes/r1-S2GOF;F8* mutants was suggested by an analysis of transverse sections through anterior r1 at E11.5. In control embryos, the roof plate (dorsal midline) was characteristically thin, i.e. only two or three cell layers deep, across a mediolateral domain five to eight cell diameters in width (Fig. 5A,A'). By contrast, in *mes/r1-S2GOF;F8* mutants at a comparable anteroposterior (AP) level, the roof plate was similarly thin but much wider than normal (Fig. 5B,B'). This region in the mutants appeared similar in width to the roof plate in more posterior sections of control and mutant embryos, where it comprised a single cell layer that was ~30 cell diameters wide (Fig. 5C-D').

We next examined gene expression patterns at earlier stages. In control embryos at E10.5, as well as in *mes/r1-S2GOF* embryos, the near circular *Fgf8* expression domain in anterior r1 is interrupted at the dorsal midline by a small group of *Fgf8*-negative roof plate cells (Fig. 5E,F; data not shown). In *mes/r1-S2GOF;F8* embryos, the *Fgf8* expression pattern appeared almost normal up to E9.5 (28 somites; Fig. 5H,I), but by E10.5 (34 somites) the *Fgf8*-negative domain in dorsal r1 was much wider than normal (Fig. 5G, compare with 5E,F). In contrast to *Fgf8*, *Bmp7* expression is a positive marker of the roof plate. In control and *mes/r1-S2GOF* embryos at E10.5, it was detected in a narrow domain in anterior r1 that progressively widened towards posterior r1 (Alder et al., 1999) (Fig. 5J,K). However, in *mes/r1-S2GOF;F8* embryos, a wider *Bmp7*-positive roof plate domain was observed in anterior r1 (Fig. 5L, compare with 5J,K).

Together, these data provide strong evidence that the roof plate had expanded laterally in anterior r1 in *mes/r1-S2GOF;F8* embryos. Fate-mapping studies in the mouse embryo have localized vermis progenitors to a small domain flanking the dorsal midline in the anterior-most region of r1 at E12.5, and there is evidence that at earlier stages these cells are likewise localized close to the dorsal midline (Sgaier et al., 2005). Thus, it appears that the region containing the vermis progenitors, which is normally positive for *Fgf8* and negative for *Bmp7* expression, has been replaced by *Fgf8*-negative *Bmp7*-positive roof plate cells in *mes/r1-S2GOF;F8* embryos. These results indicate that reducing FGF signaling to the level attained in *mes/r1-S2GOF;F8* embryos causes an expansion of the roof plate between the 28- and 34-somite stages, possibly at the expense of vermis progenitors.

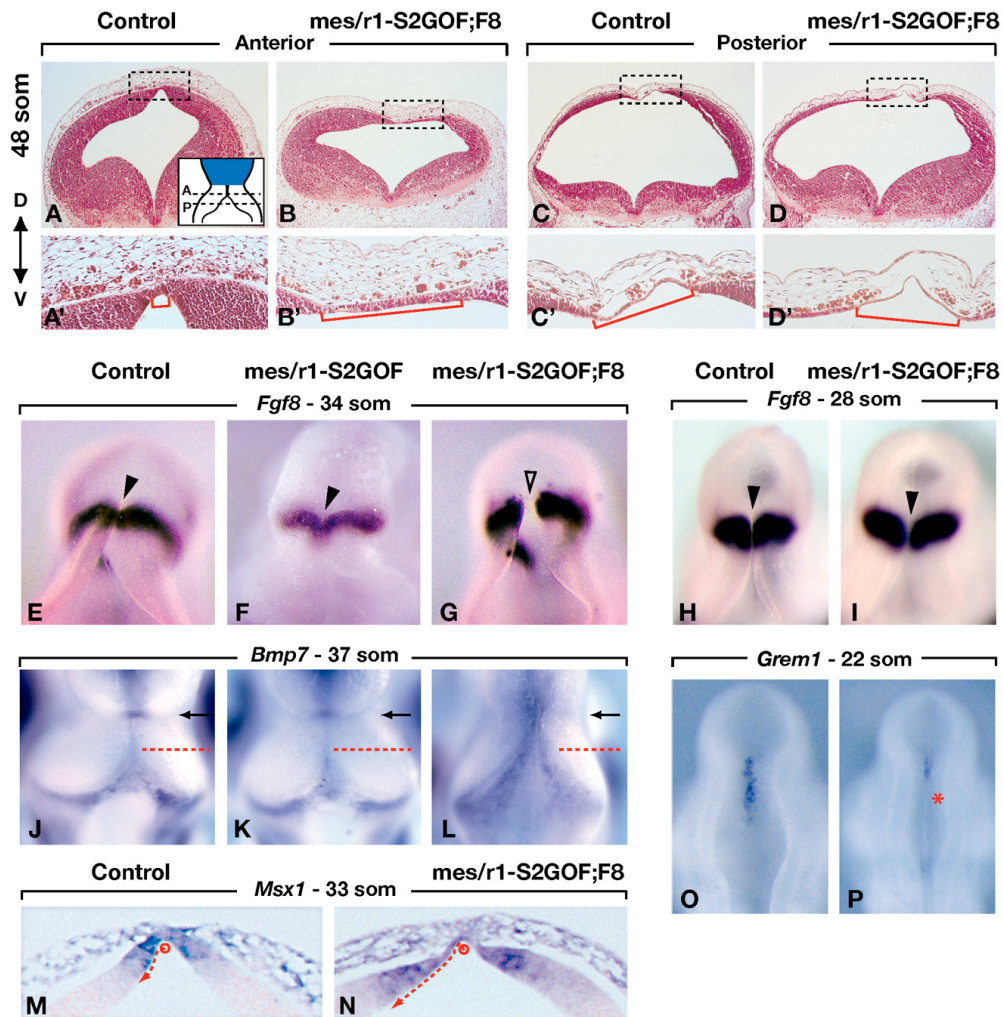


Fig. 5. The roof plate is expanded and *Grem1* expression is reduced in *mes/r1-S2GOF;F8* embryos. (A-D') Transverse sections through r1 of a control and a *mes/r1-S2GOF;F8* embryo at 48 somites (E11.75), stained with Hematoxylin and Eosin. Every third or fourth section in the series was assayed by RNA in situ hybridization with a probe for *Otx2*, to locate the posterior limit of the mesencephalon (not shown). The broken lines in the inset in A illustrate the approximate levels at which the anterior (A) and posterior (P) sections were cut, i.e. within 40-100 and 130-250 μm of the posterior limit of the *Otx2* expression domain (indicated in blue), respectively. The sections in all panels are shown at the same magnification. The regions demarcated by broken boxes in A-D are shown at fourfold higher magnification in A'-D', respectively. The mediolateral width of the dorsal midline domain in which the neuroepithelium is only two or three cell layers thick is indicated by red brackets (A'-D'). (E-L,O,P) RNA in situ hybridization assays in whole mount using the probes indicated. Dorsal views of embryos of the genotypes indicated, collected at the stages denoted. Anterior is towards the top, posterior towards the bottom. (E-I) The roof plate that bisects the *Fgf8* expression domain is indicated by arrowheads. In control and *mes/r1-S2GOF* embryos, the *Fgf8*-negative roof plate is difficult to discern; it is considerably expanded mediolaterally in the *mes/r1-S2GOF;F8* embryo (open arrowhead in G). The lateral and ventral aspect of the *Fgf8* expression domain in r1 is visible in E and G on the left side, through the roof plate. (J-L) A broken red line is drawn at the same distance posterior to the isthmic constriction at the *mes/r1* boundary (black arrow). *Bmp7* expression marks the roof plate, and the roof plate widens closer to the isthmic constriction in the *mes/r1-S2GOF;F8* embryo than in the control and *mes/r1-S2GOF* embryos. (M,N) Transverse sections through anterior r1 at approximately the same AP level as in A and B, hybridized with a probe for *Msx1*. The mediolateral extent of the *Msx1* expression domain from the center of the roof plate (open circle) is indicated by a broken red arrow. (O,P) *Grem1* expression is readily detected at the dorsal midline of r1 in the control embryo, but is barely detected in r1 of the *mes/r1-S2GOF;F8* embryo (red asterisk).

BMP target gene expression is increased and BMP antagonist gene expression is decreased in *mes/r1-S2GOF;F8* mutants

Previous studies have indicated that roof plate cells express several BMP family members in addition to *Bmp7*, and that BMP signaling is necessary and sufficient for roof plate development in the chick neural tube (Lee and Jessell, 1999; Chizhikov and Millen, 2004b; Chizhikov and Millen, 2004c; Liu et al., 2004). The transcription factor gene *Msx1* is a downstream target of BMP signaling in the dorsal neural tube, and misexpression of *Msx1* in the chick spinal

cord results in expansion of the roof plate (Liu et al., 2004). Therefore, to determine whether excess BMP signaling might be responsible for the roof plate expansion we observed in *mes/r1-S2GOF;F8* embryos at E10.5, we assayed for *Msx1* expression as a readout for BMP signaling in dorsal r1. The domain of *Msx1* expression was indeed significantly expanded mediolaterally in anterior r1 in *mes/r1-S2GOF;F8* embryos as compared with control embryos at 33 somites (Fig. 5M,N). These data support the hypothesis that a decrease in FGF signaling in r1 results in an increase in BMP signaling and expansion of the roof plate.

In considering how FGF signaling in anterior r1 could function to inhibit BMP signaling, we investigated the possibility that it might induce or maintain the expression of genes that encode secreted BMP antagonists. One such gene is gremlin 1 (*Grem1*) (Hsu et al., 1998), which is expressed in the roof plate of anterior r1 (Pearce et al., 1999; Louvi et al., 2003). We found that in control embryos at E9.25 (22 somites), *Grem1* RNA was readily detected in the roof plate and adjacent neuroepithelium (Fig. 5O, and data not shown), whereas in *mes/r1-S2GOF;F8* embryos *Grem1* expression was barely detected in anterior r1 (Fig. 5P). By contrast, *Grem1* expression was only moderately reduced in *mes/r1-S2GOF* embryos (not shown). These results suggest that a normal function of FGF signaling from the IsO is to inhibit BMP signaling in dorsal r1 via a positive effect on *Grem1* expression.

DISCUSSION

In this study, we produced the equivalent of an FGF loss-of-function allelic series specifically in *mes/r1* and examined the effects of progressively reducing FGF signaling on midbrain and cerebellum development. By recombining one copy of a conditional *Spry2* gain-of-function allele throughout *mes/r1* at ~E8.5, we obtained *mes/r1-S2GOF* mutants with a phenotype similar to that of *Fgf17^{-/-};Fgf8^{+/-}* mutants (Xu et al., 2000). When we reduced *Fgf8* gene dose in *mes/r1-S2GOF* mutants, or produced animals with two copies of the recombined *Spry2-GOF* allele, we obtained a more severe phenotype, which resembled that of embryos homozygous for an *Fgf8* hypomorphic allele (*Fgf8^{neo}*) (Chi et al., 2003). Together, these data strongly support the hypothesis that expression of the recombined *Spry2-GOF* allele results in an inhibition of signaling via FGF receptors rather than other RTKs during midbrain and cerebellum development. A dorsal *mes/r1* phenotype similar to that in *mes/r1-S2GOF;F8* embryos has also been observed following conditional inactivation of *Fgfr1* in *mes/r1* (Trokovic et al., 2003), suggesting that the FGF signaling that is affected in the *Spry2* gain-of-function mutants is primarily relayed by FGFR1.

The results of our analysis provide genetic evidence consistent with the proposal that the processes that shape the midbrain and cerebellum require distinct levels of FGF signaling (Liu et al., 1999; Sato et al., 2001; Liu et al., 2003), and further reveal that anatomically and functionally distinct regions within the midbrain and cerebellum require different levels of FGF signaling for their development. This conclusion is consistent with the results of a recent analysis showing that when *En1/En2* function, which is apparently downstream of FGF signaling from the IsO, is progressively compromised, specific functional domains of the tectum and vermis are lost in a dose-dependent manner (Sgaier et al., 2007). In addition, we present evidence that FGF signaling influences the balance between vermis and roof-plate development in anterior r1 via an effect on BMP signaling.

The effects of *Spry2* gain-of-function in *mes/r1* differ in mouse and chicken embryos

The phenotypes we observed in our mutant mice differ from those reported in chicken embryos, in which ectopic expression of *Spry2* caused cells in r1 to express *Otx2*, a marker for the mes, and to develop into midbrain tissue (Suzuki-Hirano et al., 2005). We did observe that *Otx2* expression was abnormal in *mes/r1-S2GOF;F8* embryos, in that the boundary between *Otx2*-positive and *Otx2*-negative cells was not as sharp as in control embryos and there were a few *Otx2*-positive cells scattered in r1 (see Fig. S2 in the supplementary material). However, we found no evidence that r1

cells took on a midbrain fate. Instead, misexpressing *Spry2* in *mes/r1* resulted in defects in vermis development. Although there is evidence that the forced expression of *Otx2* in r1 from E8.75 can transform anterior r1 into midbrain tissue in the mouse embryo (Broccoli et al., 1999), there is as yet no direct evidence that mouse r1 can give rise to midbrain tissue when FGF signaling is reduced. The disparity between our findings and those of Suzuki-Hirano et al. (Suzuki-Hirano et al., 2005) might be due to differences in the methods employed to obtain ectopic sprouty gene expression, i.e. sustained expression of an inherited transgene in the mouse versus transient expression of a transgene introduced by electroporation in the chicken embryo. Alternatively, it is possible that the different results reflect differences in the mechanisms that control the level of FGF signaling in mouse versus chicken brain development.

Loss of the posterior tectum caused by reducing FGF signaling can be explained by death of anterior cells and mis-specification of posterior cells as anterior tectum

A specific loss of the IC, with normal development of the SC, is a feature common to mutants in which FGF signaling is moderately reduced in *mes/r1*, including *Fgf17^{-/-};Fgf8^{+/-}* embryos (Xu et al., 2000), *Fgf8^{neo/neo}* embryos (Chi et al., 2003) and embryos in which *Fgfr1* has been inactivated in *mes/r1* (Trokovic et al., 2003), but the mechanism by which this loss occurs is not known. Death of IC progenitors is one possible explanation, as we previously showed that inactivation of *Fgf8* in *mes/r1* by the 10-somite stage results in apoptosis throughout the mes (Chi et al., 2003). However, cell death was not detected at E9.5 in the mesencephalon when *Fgfr1* was inactivated (Trokovic et al., 2003).

Here, we show that a moderate reduction in FGF signaling does cause abnormal cell death prior to E9.25, but that the dying cells are detected only in the anterior mes. To explain this localization, we propose that there is a minimum level of FGF signaling below which cells in the mes die. In normal embryos, there is sufficient FGF signaling to sustain survival, even of cells that are furthest from the source of FGFs in the IsO (Fig. 6A). However, when FGF signaling is moderately reduced, as for example in *mes/r1-S2GOF* mutants, only cells close to the IsO attain the level of FGF signaling required for survival. At early stages, when the mes is relatively small, all the cells are sufficiently close to the IsO. But as the mes increases in size and the anterior-most cells in such mutants are displaced progressively further from the IsO, they reach a point at which they are too far from the IsO to attain the level of FGF signaling required for survival, and therefore they die.

The observation that cell death is restricted to the anterior mes suggests the following explanation for the loss of the IC in mutants with reduced FGF signaling in the mes: AP cell fates have not yet been determined in the mes at the stage when the cells are dying, and the remaining posterior cells are subsequently specified as SC because of the low level of FGF signaling. Consistent with this hypothesis, it has been shown that fate changes can occur in explants of E9.5 mouse midbrains (Liu et al., 1999). Presumably, if cells in the anterior mes had died at a stage after the fate of all mes cells had been determined, a normal SC would not have formed. This model further suggests that specification of IC progenitors requires a higher level of FGF signaling than specification of SC progenitors. This idea is supported by data showing that increasing FGF signaling, by inserting beads loaded with FGF protein in the anterior mes of chicken embryos, induces anterior cells to take on a posterior fate (Martinez et al., 1999; Shamim et al., 1999).

Loss of the vermis caused by reducing FGF signaling can be explained by an increase in BMP signaling and expansion of the roofplate

A loss of the entire vermis is observed when FGF signaling is reduced to a level lower than in *Fgf17^{-/-};Fgf8^{+/-}* and *mes/r1-S2GOF* mutants. Our data indicate that abnormal cell death is not responsible for the loss of the vermis in such mutant embryos. Instead, the vermis may be absent because a specific minimum level of FGF signaling is required for specification and/or expansion of vermis progenitors (Liu et al., 2003), and that level is not attained in such mutants. Another possibility is based on our observation that the roof plate in *r1* is abnormally expanded in *mes/r1-S2GOF;F8* embryos. Although this abnormality might be secondary to a failure of vermis development,

we favor the hypothesis that the converse is true, and that the observed expansion of the roof plate is the primary cause of loss of the vermis (Fig. 6B).

The model we advocate is based on studies showing that in the spinal cord, the roof plate forms in response to BMP signaling from the adjacent epidermal ectoderm (Lee and Jessell, 1999; Chizhikov and Millen, 2004c; Chizhikov and Millen, 2005), that overexpression of *Lmx1a* in mouse *r1* is associated with increased BMP signaling and increased roof plate formation (Chizhikov et al., 2006), and that BMP signaling can be inhibited by FGF signaling in numerous developmental settings, including the forebrain (Storm et al., 2003) and midbrain (Alexandre et al., 2006). We propose that in *r1*, roof plate formation is likewise controlled by BMP signaling from the ectoderm, which in turn is inhibited by FGF signaling from the IsO. This inhibitory interaction could explain why the roof plate is normally so narrow in anterior *r1*, adjacent to the IsO where FGF ligands are produced, but is much wider in more posterior *r1*. Accordingly, when FGF signaling is sufficiently reduced, as in *mes/r1-S2GOF;F8* embryos, BMP signaling increases, and the roof plate in anterior *r1* becomes abnormally wide (Fig. 6C). In support of this idea, we found that in *mes/r1-S2GOF;F8* embryos, BMP signaling is increased, as evidenced by an expansion of the *Msx1* expression domain. Moreover, we observed that a dramatic reduction in expression of the BMP antagonist *Grem1* precedes abnormal expansion of the roof plate by ~12 hours, suggesting a molecular mechanism by which FGF signaling could exert a negative effect on BMP signaling and roof plate expansion in *r1*, because we found that roof plate development appears normal in *Grem1*-null embryos (not shown).

An important question is how might the expansion of the roof plate observed in *mes/r1-S2GOF;F8* mutants compromise vermis development? One possibility is based on the fact that the roof plate itself expresses BMPs (Alder et al., 1999; Lee and Jessell, 1999; Alexandre et al., 2006), and an increase in the size of the cell population producing these potent signaling molecules might in turn cause the nearby vermis progenitors to slow their proliferation or differentiate prematurely, leading ultimately to absence of the vermis (Alder et al., 1999; Krizhanovsky and Ben-Arie, 2006; Machold et al., 2007). Alternatively, as misexpression of the BMP effector *MSX1* results in the conversion of spinal cord neuroepithelium into roof plate (Liu et al., 2004), it is possible that the increase in *Msx1* expression in *mes/r1-S2GOF;F8* mutants functions to stimulate roof plate development at the expense of the vermis by converting vermis progenitors to a roof plate fate. Further studies will be needed to distinguish between these possibilities.

We thank Drs George Minowada, who produced the *Spry2-GOF* mouse lines and initiated the studies described here, and Benjamin Yu and Robert Hindges for helpful suggestions. We are grateful to P. Ghatpande and Monica Rodenas for excellent technical assistance. We also thank Drs Roy Sillitoe and Richard Wingate, and our laboratory colleagues for helpful comments on the manuscript. D.E. was supported by the Spanish Ministry of Health, Instituto de salud Carlos III, CIBERSAM (CB07/09/0021). This work was supported by grants from the Wellcome Trust (080470) to M.A.B. and (072111) to M.A.B. and I.M., by the Medical Research Council and a Leverhulme Trust Fellowship to I.M., by the EU research program (LSHG-CT-2004-512003 and MEIF-CT-2006-025154), the Spanish Science Program (MEC BFU2005-09085, RD06/0011/0012), the ELA Foundation Research and TV3 LA (MARATO-062232) to D.E. and S.M., and by the National Institutes of Health (R01 HD050767) to A.L.J. and (R01 CA78711) to G.R.M.

Supplementary material

Supplementary material for this article is available at <http://dev.biologists.org/cgi/content/full/135/5/889/DC1>

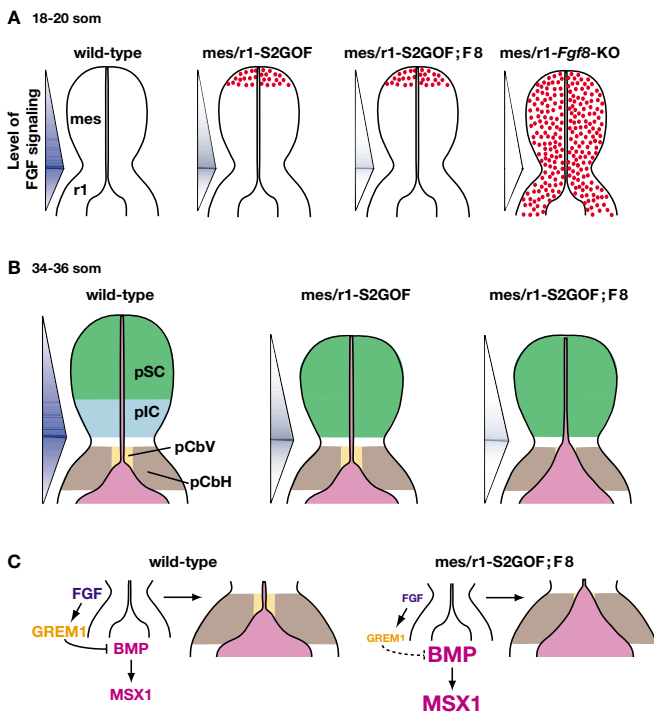


Fig. 6. A model to explain the phenotypes obtained when FGF signaling is progressively reduced in *mes/r1*. Schematic diagrams illustrate dorsal views of *mes/r1* in embryos of the genotypes indicated at the somite stages denoted. The intensity of the blue color in the triangle to the left of a diagram illustrates the level of FGF signaling. (A) The regions in which cells are dying or have already died are indicated by red stippling. (B) The regions that contain the progenitors (p) of the superior colliculus (SC), inferior colliculus (IC), cerebellar vermis (CbV) and cerebellar hemispheres (CbH) are indicated. The phenotypes observed in mutants that attain progressively lower levels of FGF signaling are illustrated. In *mes/r1-S2GOF* embryos, the anterior *mes* has been lost, and the surviving posterior cells are specified to an anterior (SC) fate. Consequently the IC does not develop. In *mes/r1-S2GOF;F8* embryos, the effects on the *mes* are similar and, in addition, the vermis fails to develop because roof plate (RP) expansion in *r1* results in a loss of CbV progenitors. (C) In the wild-type embryo, FGF signaling induces/maintains the expression of *Grem1*, which functions to inhibit BMP signaling and expression of the BMP effector *MSX1*. This pathway maintains the normal balance of vermis and roof plate development. In the *mes/r1-S2GOF;F8* embryo, the reduction in the level of FGF signaling results in a severe reduction in *Grem1* expression. In the absence of this antagonist, the level of BMP signaling and therefore *MSX1* expression increases and an expanded roof plate develops where the vermis progenitors normally reside.

References

- Alder, J., Lee, K. J., Jessell, T. M. and Hatten, M. E.** (1999). Generation of cerebellar granule neurons in vivo by transplantation of BMP-treated neural progenitor cells. *Nat. Neurosci.* **2**, 535-540.
- Alexandre, P., Bachy, I., Marcou, M. and Wassef, M.** (2006). Positive and negative regulations by FGF8 contribute to midbrain roof plate developmental plasticity. *Development* **133**, 2905-2913.
- Broccoli, V., Boncinelli, E. and Wurst, W.** (1999). The caudal limit of Otx2 expression positions the isthmus organizer. *Nature* **401**, 164-168.
- Calmont, A., Wandzioch, E., Tremblay, K. D., Minowada, G., Kaestner, K. H., Martin, G. R. and Zaret, K. S.** (2006). An FGF response pathway that mediates hepatic gene induction in embryonic endoderm cells. *Dev. Cell* **11**, 339-348.
- Casci, T., Vinos, J. and Freeman, M.** (1999). Sprouty, an intracellular inhibitor of Ras signaling. *Cell* **96**, 655-665.
- Chi, C. L., Martinez, S., Wurst, W. and Martin, G. R.** (2003). The isthmus organizer signal FGF8 is required for cell survival in the prospective midbrain and cerebellum. *Development* **130**, 2633-2644.
- Chizhikov, V. V. and Millen, K. J.** (2004a). Control of roof plate development and signaling by Lmx1b in the caudal vertebrate CNS. *J. Neurosci.* **24**, 5694-5703.
- Chizhikov, V. V. and Millen, K. J.** (2004b). Control of roof plate formation by Lmx1a in the developing spinal cord. *Development* **131**, 2693-2705.
- Chizhikov, V. V. and Millen, K. J.** (2004c). Mechanisms of roof plate formation in the vertebrate CNS. *Nat. Rev. Neurosci.* **5**, 808-812.
- Chizhikov, V. V. and Millen, K. J.** (2005). Roof plate-dependent patterning of the vertebrate dorsal central nervous system. *Dev. Biol.* **277**, 287-295.
- Chizhikov, V. V., Lindgren, A. G., Currle, D. S., Rose, M. F., Monuki, E. S. and Millen, K. J.** (2006). The roof plate regulates cerebellar cell-type specification and proliferation. *Development* **133**, 2793-2804.
- Crossley, P. H. and Martin, G. R.** (1995). The mouse Fgf8 gene encodes a family of polypeptides and is expressed in regions that direct outgrowth and patterning in the developing embryo. *Development* **121**, 439-451.
- Crossley, P. H., Martinez, S. and Martin, G. R.** (1996). Midbrain development induced by FGF8 in the chick embryo. *Nature* **380**, 66-68.
- Echevarria, D., Vieira, C., Gimeno, L. and Martinez, S.** (2003). Neuroepithelial secondary organizers and cell fate specification in the developing brain. *Brain Res. Brain Res. Rev.* **43**, 179-191.
- Friedrich, G. and Soriano, P.** (1991). Promoter traps in embryonic stem cells: a genetic screen to identify and mutate developmental genes in mice. *Genes Dev.* **5**, 1513-1523.
- Furthauer, M., Reifers, F., Brand, M., Thisse, B. and Thisse, C.** (2001). sprouty4 acts in vivo as a feedback-induced antagonist of FGF signaling in zebrafish. *Development* **128**, 2175-2186.
- Grieshammer, U., Cebrian, C., Ilagan, R., Meyers, E., Herzlinger, D. and Martin, G. R.** (2005). FGF8 is required for cell survival at distinct stages of nephrogenesis and for regulation of gene expression in nascent nephrons. *Development* **132**, 3847-3857.
- Hacohen, N., Kramer, S., Sutherland, D., Hiromi, Y. and Krasnow, M. A.** (1998). sprouty encodes a novel antagonist of FGF signaling that patterns apical branching of the Drosophila airways. *Cell* **92**, 253-263.
- Hsu, D. R., Economides, A. N., Wang, X., Eimon, P. M. and Harland, R. M.** (1998). The Xenopus dorsalizing factor Gremlin identifies a novel family of secreted proteins that antagonize BMP activities. *Mol. Cell* **1**, 673-683.
- Inouye, M. and Oda, S. I.** (1980). Strain-specific variations in the folial pattern of the mouse cerebellum. *J. Comp. Neurol.* **190**, 357-362.
- Itoh, N. and Ornitz, D. M.** (2004). Evolution of the Fgf and Fgfr gene families. *Trends Genet.* **20**, 563-569.
- Kimmel, R. A., Turnbull, D. H., Blanquet, V., Wurst, W., Loomis, C. A. and Joyner, A. L.** (2000). Two lineage boundaries coordinate vertebrate apical ectodermal ridge formation. *Genes Dev.* **14**, 1377-1389.
- Krizhanovskiy, V. and Ben-Arie, N.** (2006). A novel role for the choroid plexus in BMP-mediated inhibition of differentiation of cerebellar neural progenitors. *Mech. Dev.* **123**, 67-75.
- Lagares, C., Caballero-Bleda, M., Fernandez, B. and Puelles, L.** (1994). Reciprocal connections between the rabbit supragenulate pretectal nucleus and the superior colliculus: tracer study with horseradish peroxidase and fluorogold. *Vis. Neurosci.* **11**, 347-353.
- Lee, K. J. and Jessell, T. M.** (1999). The specification of dorsal cell fates in the vertebrate central nervous system. *Annu. Rev. Neurosci.* **22**, 261-294.
- Lee, S. M., Danielian, P. S., Fritsch, B. and McMahon, A. P.** (1997). Evidence that FGF8 signalling from the midbrain-hindbrain junction regulates growth and polarity in the developing midbrain. *Development* **124**, 959-969.
- Li, J. Y., Lao, Z. and Joyner, A. L.** (2002). Changing requirements for Gbx2 in development of the cerebellum and maintenance of the mid/hindbrain organizer. *Neuron* **36**, 31-43.
- Liu, A., Losos, K. and Joyner, A. L.** (1999). FGF8 can activate Gbx2 and transform regions of the rostral mouse brain into a hindbrain fate. *Development* **126**, 4827-4838.
- Liu, A., Li, J. Y., Bromleigh, C., Lao, Z., Niswander, L. A. and Joyner, A. L.** (2003). FGF17b and FGF18 have different midbrain regulatory properties from FGF8b or activated FGF receptors. *Development* **130**, 6175-6185.
- Liu, Y., Helms, A. W. and Johnson, J. E.** (2004). Distinct activities of Msx1 and Msx3 in dorsal neural tube development. *Development* **131**, 1017-1028.
- Louvi, A., Alexandre, P., Metin, C., Wurst, W. and Wassef, M.** (2003). The isthmus neuroepithelium is essential for cerebellar midline fusion. *Development* **130**, 5319-5330.
- Lu, P., Minowada, G. and Martin, G. R.** (2006). Increasing Fgf4 expression in the mouse limb bud causes polysyndactyly and rescues the skeletal defects that result from loss of Fgf8 function. *Development* **133**, 33-42.
- Machold, R. P., Kittell, D. J. and Fishell, G. J.** (2007). Antagonism between Notch and bone morphogenetic protein receptor signaling regulates neurogenesis in the cerebellar rhombic lip. *Neural Dev.* **2**, 5.
- Martinez, S., Crossley, P. H., Cobos, I., Rubenstein, J. L. and Martin, G. R.** (1999). FGF8 induces formation of an ectopic isthmus organizer and isthmocerebellar development via a repressive effect on Otx2 expression. *Development* **126**, 1189-1200.
- Mason, J. M., Morrison, D. J., Basson, M. A. and Licht, J. D.** (2006). Sprouty proteins: multifaceted negative-feedback regulators of receptor tyrosine kinase signaling. *Trends Cell Biol.* **16**, 45-54.
- Meyers, E. N., Lewandoski, M. and Martin, G. R.** (1998). An Fgf8 mutant allelic series generated by Cre- and Flp-mediated recombination. *Nat. Genet.* **18**, 136-141.
- Millonig, J. H., Millen, K. J. and Hatten, M. E.** (2000). The mouse Dreher gene Lmx1a controls formation of the roof plate in the vertebrate CNS. *Nature* **403**, 764-769.
- Minowada, G., Jarvis, L. A., Chi, C. L., Neubuser, A., Sun, X., Hacohen, N., Krasnow, M. A. and Martin, G. R.** (1999). Vertebrate Sprouty genes are induced by FGF signaling and can cause chondrodysplasia when overexpressed. *Development* **126**, 4465-4475.
- Nakamura, H.** (2001). Regionalisation and acquisition of polarity in the optic tectum. *Prog. Neurobiol.* **65**, 473-488.
- Nakamura, H., Katahira, T., Matsunaga, E. and Sato, T.** (2005). Isthmus organizer for midbrain and hindbrain development. *Brain Res. Brain Res. Rev.* **49**, 120-126.
- Olsen, S. K., Li, J. Y., Bromleigh, C., Eliseenkova, A. V., Ibrahim, O. A., Lao, Z., Zhang, F., Linhardt, R. J., Joyner, A. L. and Mohammadi, M.** (2006). Structural basis by which alternative splicing modulates the organizer activity of FGF8 in the brain. *Genes Dev.* **20**, 185-198.
- Partanen, J.** (2007). FGF signalling pathways in development of the midbrain and anterior hindbrain. *J. Neurochem.* **101**, 1185-1193.
- Pearce, J. J., Penny, G. and Rossant, J.** (1999). A mouse cerberus/Dan-related gene family. *Dev. Biol.* **209**, 98-110.
- Raible, F. and Brand, M.** (2004). Divide et Impera: the midbrain-hindbrain boundary and its organizer. *Trends Neurosci.* **27**, 727-734.
- Sato, T., Araki, I. and Nakamura, H.** (2001). Inductive signal and tissue responsiveness defining the tectum and the cerebellum. *Development* **128**, 2461-2469.
- Sgaier, S. K., Millet, S., Villanueva, M. P., Berenshteyn, F., Song, C. and Joyner, A. L.** (2005). Morphogenetic and cellular movements that shape the mouse cerebellum; insights from genetic fate mapping. *Neuron* **45**, 27-40.
- Sgaier, S. K., Lao, Z., Villanueva, M. P., Berenshteyn, F., Stephen, D., Turnbull, R. K. and Joyner, A. L.** (2007). Genetic subdivision of the tectum and cerebellum into functionally related regions based on differential sensitivity to engrailed proteins. *Development* **134**, 2325-2335.
- Shamim, H., Mahmood, R., Logan, C., Doherty, P., Lumsden, A. and Mason, I.** (1999). Sequential roles for Fgf4, En1 and Fgf8 in specification and regionalisation of the midbrain. *Development* **126**, 945-959.
- Sillitoe, R. V. and Joyner, A. L.** (2007). Morphology, molecular codes, and circuitry produce the three-dimensional complexity of the cerebellum. *Annu. Rev. Cell Dev. Biol.* **23**, 549-577.
- Storm, E. E., Rubenstein, J. L. and Martin, G. R.** (2003). Dosage of Fgf8 determines whether cell survival is positively or negatively regulated in the developing forebrain. *Proc. Natl. Acad. Sci. USA* **100**, 1757-1762.
- Sun, X., Meyers, E. N., Lewandoski, M. and Martin, G. R.** (1999). Targeted disruption of Fgf8 causes failure of cell migration in the gastrulating mouse embryo. *Genes Dev.* **13**, 1834-1846.
- Suzuki-Hirano, A., Sato, T. and Nakamura, H.** (2005). Regulation of isthmus FGF8 signal by sprouty2. *Development* **132**, 257-265.
- Trokovic, R., Trokovic, N., Hernessniemi, S., Pirvola, U., Vogt Weisenhorn, D. M., Rossant, J., McMahon, A. P., Wurst, W. and Partanen, J.** (2003). FGFR1 is independently required in both developing mid- and hindbrain for sustained response to isthmus signals. *EMBO J.* **22**, 1811-1823.
- Xu, J., Liu, Z. and Ornitz, D. M.** (2000). Temporal and spatial gradients of Fgf8 and Fgf17 regulate proliferation and differentiation of midline cerebellar structures. *Development* **127**, 1833-1843.
- Zervas, M., Blaess, S. and Joyner, A. L.** (2005). Classical embryological studies and modern genetic analysis of midbrain and cerebellum development. *Curr. Top. Dev. Biol.* **69**, 101-138.
- Zhang, X., Ibrahim, O. A., Olsen, S. K., Umehori, H., Mohammadi, M. and Ornitz, D. M.** (2006). Receptor specificity of the fibroblast growth factor family. The complete mammalian FGF family. *J. Biol. Chem.* **281**, 15694-15700.